



Delft University of Technology  
Faculty of Applied Sciences

Predicting the start of cloud formation over sea,  
using the mixed layer model

BACHELOR OF SCIENCE THESIS

by

Joost Klip

Delft, The Netherlands  
October 2011





Bachelor of Science Thesis

**“Predicting the start of cloud formation over sea,  
using the mixed layer model”**

JOOST KLIP

Delft University of Technology

**Supervisor**

Dr. S.R. de Roode

**Graduation committee**

J.J. van der Dussen Msc.

Ir. J.J.J. Gillissen

October, 2011

Delft



# Abstract

In order to improve climate models, much research has been done to the occurrence and the behaviour of clouds. To this end it is necessary to obtain more knowledge about the conditions under which a clear sky becomes cloudy. The aim of this thesis is to predict the start of cloud formation inside a clear atmospheric boundary layer, which is advected over the ocean from the subtropics to the tropics by the trade winds.

To calculate the evolution of the boundary layer the Mixed Layer Model is used. Using this model it is possible to calculate the evolution of the average values of the temperature, the pressure and the humidity inside the boundary layer, without calculating the actual motion of the air. This significantly reduces calculation time.

The conservation equations are presented and the development of the boundary layer and its interaction with the rest of the atmosphere is introduced. Using those two the model equations of the Mixed layer Model are derived. Together with the model equations some parameterizations are given to close the system.

It is known that the transition from the boundary layer to the layer above it, is characterized by a sudden increase of the temperature and a sudden decrease of humidity, called the inversion. The magnitudes of the increases in temperature ( $\Delta\theta$ ) and the humidity ( $\Delta q_t$ ) play an important role in the formation of clouds. The main topic of investigation is the influence of the initial values of  $\Delta\theta$  and  $\Delta q_t$  on the time after which clouds start to form. Next to these two the influence on three other variables is investigated. The variables investigated are the initial inversion height, the wind speed and the large scale divergence.

We have shown that as  $\Delta\theta$  gets larger cloud start to form earlier, while as  $\Delta q_t$  gets larger cloud formation starts later. Furthermore the lower the initial inversion height the later cloud formation starts, if the initial inversion height is chosen low enough no clouds occur at all. The influence of the wind speed turns out to be more or less the opposite of the influence of the large scale divergence. More wind makes cloud formation start sooner, while more divergence tends to delay cloud formation.



# Contents

<b>Abstract</b>	<b>v</b>
<b>1 Introduction</b>	<b>1</b>
<b>2 Theory</b>	<b>3</b>
2.1 Basic meteorological variables . . . . .	3
2.1.1 Specific humidity . . . . .	3
2.1.2 Potential temperature . . . . .	3
2.2 The conservation equations . . . . .	5
2.3 Boundary layer dynamics . . . . .	7
2.3.1 The Hadley circulation . . . . .	7
2.3.2 The inversion jump . . . . .	8
<b>3 Modeling</b>	<b>11</b>
3.1 Model equations . . . . .	11
3.2 Parameterizations . . . . .	13
3.3 Model parameters and initial conditions . . . . .	13
<b>4 Results</b>	<b>17</b>
4.1 The influence of the initial inversion height . . . . .	18
4.2 The influence of the wind speed . . . . .	23
4.3 The influence of the large scale divergence . . . . .	29
<b>5 Conclusion</b>	<b>31</b>
<b>Bibliography</b>	<b>33</b>
<b>A Validation</b>	<b>35</b>
A.1 The Nieuwstadt Case . . . . .	35
A.2 Another analytical solution . . . . .	36





# Chapter 1

## Introduction

In the last few decades concerns have risen about the changing climate and its consequences. One of the major problems in today's climate models is the uncertainty in the influence clouds have on the climate. Also the desire to make weather forecasts more accurate requires more knowledge about the occurrence of clouds, as clouds provide rain, block sunlight at daytime and prevent cooling of the earth surface at nighttime. Therefore much research is done to the formation and behaviour of clouds. In cloud modeling two major modeling methods are used. The first method is Large Eddy Simulation. This method calculates the cloud dynamics rather detailed. The other model is the Mixed Layer Model(MLM). It describes the atmospheric boundary layer, which is the lowest atmospheric layer, in terms of temperature, pressure and humidity, without calculating the motion of the air. The fact that the motion of the air is not calculated makes the model relatively simple and thus cheap in terms of computing time. A limitation is that the only spatial dimension that plays a role in the model is the height. But the model is capable of calculating the temperature, the pressure and the humidity as a function of time and height and thus, with the help of thermodynamics, it is capable to calculate the amount of liquid water (and ice) as a function of height. At heights where liquid water (or even ice) is present we can conclude that clouds occur. So with the MLM it is possible to calculate on which heights cloud formation is to be expected. In this thesis the MLM is used to investigate the effect of the initial temperature jump and the initial moisture jump across the inversion on the time scale at which clouds start to form. The environment investigated is an environment above the ocean between the equator and the so-called horse latitudes, these horse latitudes are 30-35 degrees north and south.



# Chapter 2

## Theory

In this chapter the behaviour of the boundary layer and its interaction with the rest of the atmosphere is introduced. To understand this behaviour and the interactions some variables that make calculations in meteorology more convenient are introduced first. Afterwards the behaviour of the boundary layer is described using the general conservation equations. Lastly the development of the boundary layer and its interaction with the rest of the atmosphere is introduced.

### 2.1 Basic meteorological variables

#### 2.1.1 Specific humidity

To be able to understand the equations which describe the mixed layer some basic variables, common in meteorology, have to be introduced. The first one is the total specific humidity  $q_t$ . It is defined as the mass fraction of the total amount of water in a parcel of air:

$$q_t = \frac{m_w}{m}. \quad (2.1)$$

Here  $m_w$  is the mass of the water inside the parcel of air and  $m$  is the total mass of the parcel:  $m = m_w + m_d$  where  $m_d$  is the mass of dry air. In general the specific humidity can consist of three fractions: an ice fraction  $q_i$ ; a liquid fraction  $q_l$  and a vapour fraction  $q_v$ . Because in this thesis only the situation of clear sky is studied the only fraction present in the air is the vapour fraction so  $q_t = q_v$ . To be able to calculate whether a cloud occurs we need another variable: the specific humidity of saturation ( $q_{sat}$ ). It is given by the relationship of Clausius-Clapeyron:

$$q_{sat} = \frac{e_{sat}}{p - e_{sat}}. \quad (2.2)$$

In this formula  $p$  is the pressure and the function  $e_{sat}$  is given by:

$$e_{sat} = 610.087e^{\frac{17.2649(T-273.16)}{T-35.86}}. \quad (2.3)$$

Here we see that  $e_{sat}$  strongly depends on the temperature. In the next subsection it will be made clear how the variable temperature is treated in meteorology.

#### 2.1.2 Potential temperature

It is commonly known that in the atmosphere the temperature decreases with the height. In meteorology a variable is used which is corrected for this, the potential temperature  $\theta$ . First we

try to find out what happens to the temperature of a parcel of dry air which is moved along the  $z$ -axis adiabatically. To do this we start with:

$$\frac{dp}{dz} = -\rho g. \quad (2.4)$$

Here  $\rho$  is the density of dry air and  $g$  is the gravitational acceleration. From thermodynamics we have the differential relation  $dh = Tds + vdp$  where  $h$ ,  $s$  and  $v$  are the specific enthalpy; the specific entropy and the specific volume respectively. The process is adiabatic so  $ds = 0$ . Furthermore the enthalpy is related to the temperature through  $dh = c_p dT$ , where  $c_p$  is the specific heat at constant pressure, and  $v = \frac{1}{\rho}$ . So now we have:

$$c_p dT = \frac{dp}{\rho}. \quad (2.5)$$

Combining equations (2.4) and (2.5) gives:

$$dT = -\frac{gdz}{c_p}. \quad (2.6)$$

Integrating this equation yields:

$$T = T_0 - \frac{gz}{c_p}. \quad (2.7)$$

The variable  $T_0$  is, as can be easily seen in (2.7), the temperature a parcel of air would have at the bottom of the mixed layer (height  $z = 0$ ). Using the ideal gas law:

$$\rho = \frac{p}{TR_d}, \quad (2.8)$$

where  $R_d$  is the gas specific constant of dry air, the pressure in the parcel of air can be related to its height.

Combining equations (2.4), (2.7) and (2.8) we get:

$$\frac{dp}{dz} = -\frac{g}{R_d \left( T_0 - \frac{gz}{c_p} \right)} p. \quad (2.9)$$

This can also be written as:

$$\frac{dp}{p} = -\frac{gdz}{R_d \left( T_0 - \frac{gz}{c_p} \right)}. \quad (2.10)$$

Using the fact that  $\int \frac{a}{b+cx} dx = \frac{a}{c} \ln(b+cx)$  this gives:

$$p = p_0 T_0^{-\frac{c_p}{R_d}} \left( T_0 - \frac{gz}{c_p} \right)^{\frac{c_p}{R_d}}, \quad (2.11)$$

where  $p_0$  is a reference pressure. With the fact that  $T = T_0 - \frac{gz}{c_p}$  this can be rewritten to:

$$\frac{T}{T_0} = \left( \frac{p}{p_0} \right)^{\frac{R_d}{c_p}}. \quad (2.12)$$

Here  $\frac{T}{T_0}$  is known as the Exner function, which is denoted by  $\Pi(p)$ . In meteorology it is common to use  $p_0 = 10^5 \text{Pa}$  as reference pressure. When using this reference pressure the reference temperature  $T_0$  is called the potential temperature and is denoted by  $\theta$ . So now we have:

$$\Pi = \frac{T}{\theta}. \quad (2.13)$$

Equations (2.8) up to (2.13) apply for dry air only. It is known that water vapour has less density than dry air, so the specific humidity has influence on the buoyancy of air. Looking at (2.8) we must conclude that moist air has a larger gas constant. In meteorology it is common to adapt the value of the temperature instead of using a gas constant which is not really constant but a function of the total water content ( $q_t$ ). The adapted value of the temperature is called the virtual temperature. It is denoted by a subscript v. This virtual temperature is defined as the temperature a parcel of dry air with the same density and pressure would have. The formal derivation of this virtual temperature can be found in Stull (1993):

$$T_v = (1 + 0.61q_t)T. \quad (2.14)$$

Dividing this virtual temperature by the Exner function gives the virtual potential temperature:

$$\theta_v = \frac{T_v}{\Pi}. \quad (2.15)$$

## 2.2 The conservation equations

The starting point to find the basic equations of the mixed layer model is the set of conservation equations:

$$\frac{\partial \psi}{\partial t} + \frac{\partial u_j \psi}{\partial x_j} = 0. \quad (2.16)$$

In this equation  $x_j$  represents the Cartesian coordinates,  $\vec{x} = (x, y, z)$ ,  $\psi$  is any conserved quantity (such as  $\theta$ ,  $\theta_v$  and  $q_t$ ),  $u_j$  is the  $j^{\text{th}}$  component of the wind velocity and  $\vec{u} = (u, v, w)$ . Equation (2.16) is averaged using Reynolds averaging, this means splitting the variables in a mean part  $\bar{\psi}$  and a deviation from the mean called the turbulent part  $\psi'$ , so that  $\psi = \bar{\psi} + \psi'$ . Averaging (2.16):

$$\frac{\partial \bar{\psi}}{\partial t} + \frac{\partial \overline{u_j \psi}}{\partial x_j} = 0 \quad (2.17)$$

In the mixed layer model it is assumed that the atmosphere is horizontally homogeneous. Using this assumption and (2.17) van der Dussen (2009) derived that:

$$\frac{\partial \bar{\psi}}{\partial t} + \bar{w} \frac{\partial \bar{\psi}}{\partial z} = -\frac{\partial \overline{w' \psi'}}{\partial z}. \quad (2.18)$$

Here  $\overline{w' \psi'}$  denotes the turbulent flux of  $\psi$ . Another assumption of the mixed layer model is that any conserved quantity is spread uniformly over the boundary layer. The reasoning behind this assumption is that the sea surface is always a lot warmer than the atmosphere. This temperature difference between the sea surface and the atmosphere induces a lot of turbulence inside the boundary layer. It is assumed that the turbulent transport evens out gradients in conserved quantities quickly. This is the reason why the boundary layer is also called the (well) mixed layer. This means that conserved quantities don't have vertical gradients. So the second term of (2.18) is zero giving:

$$\frac{\partial \bar{\psi}}{\partial t} = -\frac{\partial \overline{w' \psi'}}{\partial z}. \quad (2.19)$$

Futhermore a quasi steady state situation is assumed so that  $\frac{\partial}{\partial t} \frac{\partial \bar{\psi}}{\partial z} = 0$  combining this with (2.19) gives:

$$\frac{\partial}{\partial z} \frac{\partial \overline{w'\psi'}}{\partial z} = 0. \quad (2.20)$$

This implies that the fluxes are a linear function of the height, so that (2.19) can be rewritten to:

$$\frac{d\bar{\psi}}{dt} = - \frac{\overline{w'\psi'_{z_i}} - \overline{w'\psi'_0}}{z_i}. \quad (2.21)$$

Where  $z_i$  the thickness of the mixed layer,  $\overline{w'\psi'_{z_i}}$  is the flux at the top of the mixed layer and  $\overline{w'\psi'_0}$  the surface flux. In the rest of this thesis the value of a Reynolds averaged quantity  $\bar{\psi}$  inside the mixed layer will be denoted by  $\psi_{ml}$ .

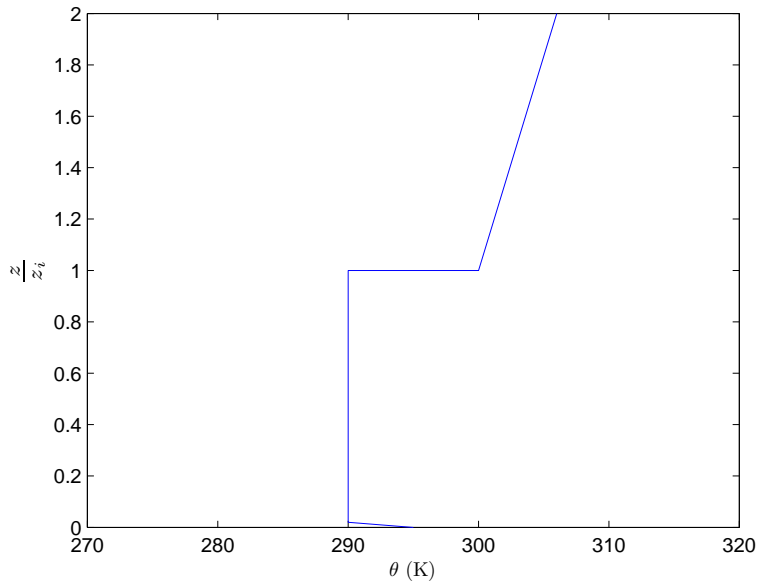


Figure 2.1: The profile of  $\theta$ .

## 2.3 Boundary layer dynamics

In this subsection the interaction between the boundary layer and the rest of the atmosphere is briefly introduced. A more detailed description can be found in van der Dussen (2009).

### 2.3.1 The Hadley circulation

To understand this interaction we have to look at the global circulation of the air inside the atmosphere. The circulation is induced because at the equator, where insolation is strongest, air is heated up and transported upwards and loses its moisture due to rain. This air is transported north- and southwards and comes down around the horse-latitudes (30-35 degrees north and south). The air is transported back by the so called trade winds. This air circulation is called the Hadley Circulation. A schematic picture of this circulation is given in figure 2.2.

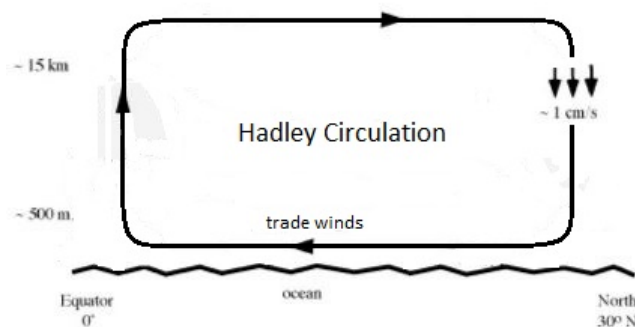


Figure 2.2: A schematic picture of the Hadley circulation.

So around the horse latitudes relatively warm and dry air is advected downward, this downward advection is called subsidence. This makes that the potential temperature increases with height. In this thesis it is assumed that the potential temperature increases linearly with height in what we call "free atmosphere". It is known from measurements, that the potential temperature increases with 5 to 6 K/km. A consequence of this increase in potential temperature is that if a parcel of is moved upwards adiabatically inside free atmosphere, its temperature will become lower than the temperature of its environment. Therefore it will fall back to its original height. Thus the free atmosphere has a laminar structure. At the surface the laminar structure is disturbed due to a large temperature difference between the surface and the air above it. This temperature difference generates a lot of upwards turbulent advection of air. The only way the air is decelerated is when it encounters air of a higher temperature. This will happen because the potential temperature in free atmosphere only increases with height. So the air advected from the surface will be able to reach just a certain height. Just below this height the potential temperature will be much lower than just above it. So across the interface from the boundary layer to the free atmosphere the temperature shows a very sharp increase. This interface, although it is in reality in the order of 50m thick, is modelled as an infinitesimal thin layer called the inversion. As mentioned earlier the turbulent character of the boundary layer gives rise to the assumption that local gradients of any conserved quantity are evenend out, this means that the value of any conserved quantity is in good approximation constant throughout the boundary layer. An example of such a conserved quantity is the potential temperature.

So the potential temperature profile in the atmosphere behaves as follows:

1. The boundary layer in which the potential temperature is constant
2. The inversion, a sharp increase in potential temperature
3. Free atmosphere where the potential temperature increases with  $5 - 6\text{K/km}$

A schematic plot of this potential temperature profile is given in figure 2.1.

### 2.3.2 The inversion jump

The existence of the inversion jump makes transport across the inversion jump difficult because air that moves from the boundary layer into free atmosphere encounters air of a much higher temperature, so it will get a large deceleration. There is however some transport across the inversion because some of the air inside the boundary layer will have enough upward velocity to cross the inversion. Above the inversion it will encounter warmer, and thus less dense, air so it will fall back into the boundary layer. Falling back into the boundary layer it will drag some of the warm, dry air from the free atmosphere into the boundary layer. This process is called entrainment. When air is entrained into the boundary layer the total amount of air inside the boundary layer increases while the density of the air remains practically the same. This means that the boundary layer must get thicker, so the inversion height must increase. Another effect that influences the motion of the inversion is the subsidence, which pushes the inversion downwards. Both the entrainment rate and the subsidence are expressed as speeds so that the change of the position of the inversion is the sum of these speeds:

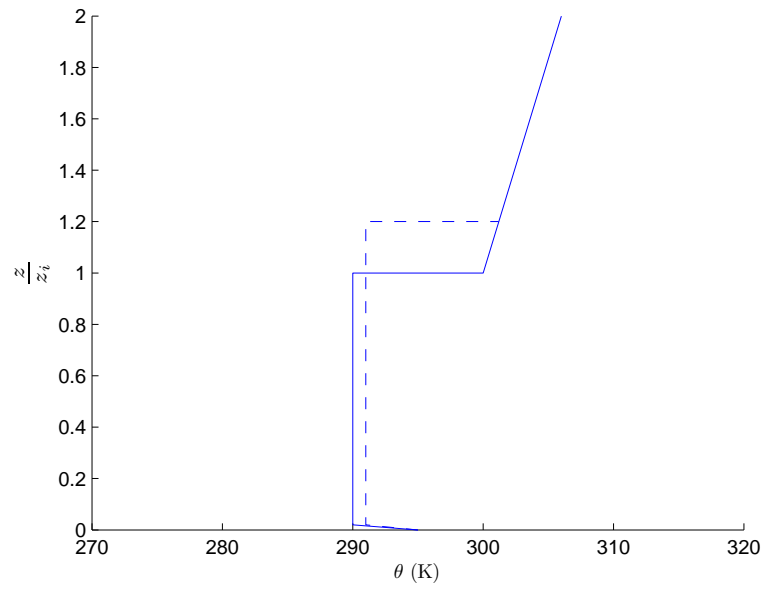
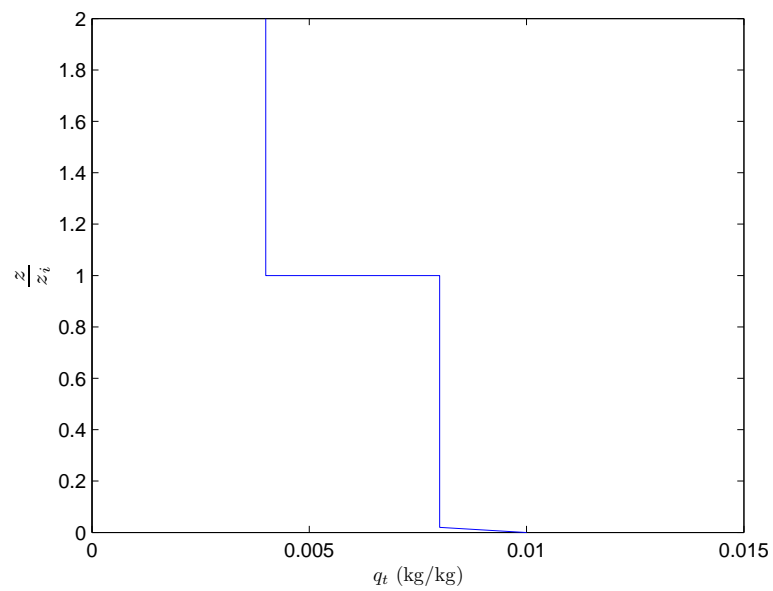
$$\frac{dz_i}{dt} = w_e + w_{subs}. \quad (2.22)$$

Here  $w_e$  is the entrainment rate,  $w_{subs}$  is the subsidence speed and  $z_i$  is the inversion height. The temperature jump across the inversion is easily calculated with  $\Delta\theta = \theta_{fa}|_{z=z_i^+} - \theta_{ml}$  where  $\theta_{ml}$  is the potential temperature inside the mixed layer and  $\theta_{fa}|_{z=z_i^+}$  is the potential temperature just above the inversion, it will be denoted by  $\theta_{fa}$  in the rest of this thesis. This potential temperature depends on the inversion height, as can be seen in figure 2.3. Assuming that after a certain time  $t_1$  the inversion height has moved from  $z_i(0)$  to  $z_i(t_1)$  it is easily calculated that in the final situation  $\theta_{fa}(z_i(t_1)) = \theta_{fa}(z_i(0)) + \Gamma_\theta(z_i(t_1) - z_i(0))$  so that:

$$\Delta\theta = \theta_{fa}(z_i(0)) + \Gamma_\theta(z_i(t_1) - z_i(0)) - \theta_{ml}. \quad (2.23)$$

The profile of the specific humidity looks similar. We know that the specific humidity is a conserved quantity so it is constant throughout the boundary layer. In free atmosphere the Hadley circulation causes a downward advection of relatively dry air, so that the free atmosphere is dryer than the boundary layer. In this thesis the specific humidity in free atmosphere ( $q_{t,fa}$ ) is assumed to be constant in both height and time. A plot of the profile of the specific humidity is given in figure 2.4. The jump in the humidity is calculated as:  $\Delta q_t = q_{t,fa} - q_{t,ml}$  where  $q_{t,ml}$  is the specific humidity inside the mixed layer.



Figure 2.3: The profile of  $\theta$ .Figure 2.4: The profile of  $q_t$ .



## Chapter 3

# Modeling

In the previous chapter two conserved variables have been introduced, namely the potential temperature and the total specific humidity. In this chapter it will be shown that those two variables together with the inversion height determine whether clouds occur. The equations that determine the evolution of those three variables, the model equations, will also be presented in this chapter. In order to close the obtained system of equations, parameterizations will be given in section 2 and model parameters and initial conditions will be given in section 3.

### 3.1 Model equations

The purpose of the model used in this thesis is to find out under which circumstances clouds will form inside the boundary layer and if so, how long it takes before they start forming. It is clear that a cloud starts to form when somewhere the air reaches the saturation point, this means  $q_t = q_{sat}$ . In the previous section we made the assumption that conserved variables, such as  $q_t$  are spatially independent inside the boundary layer. So the position at which a cloud starts to form is the position at which  $q_{sat}$  is lowest. equations (2.2) and (2.3) show that  $q_{sat}$  depends on the absolute temperature  $T$  and the pressure  $p$ . Using equations (2.7) and (2.13) both  $T$  and  $p$  can be written in terms of  $p_0$ ,  $\theta$  and  $z$ . So  $q_{sat}$  can also be expressed in terms of these three variables. In figure 3.1  $q_{sat}$  is plotted as a function of  $T$  at several values of  $p$ .

Figure 3.1 makes clear that  $q_{sat}$  depends on  $T$  quite strongly while it hardly depends on  $p$ . Knowing that  $T$  decreases with height according to (2.7) and that the free atmosphere is warmer and dryer than the boundary layer. It can be concluded that saturation will occur earliest at the top of the boundary layer. To find out how much time it takes before saturation is reached the evolution of  $q_{sat}$  and  $q_t$  must be calculated. Because saturation will occur earliest at the top of the boundary layer we are only interested in the value of  $q_{sat}$  at the top, which is denoted by  $q_{sat,top}$ . In section 2 we have seen that  $q_{sat,top}$  depends on  $\theta_{ml}$  and  $z_i$  only. The fact that all advection processes in the atmosphere are buoyancy driven complicates direct calculations with  $\theta_{ml}$ , therefore the adapted value  $\theta_{v,ml}$  will be used. The evolution of  $\theta_{v,ml}$  and  $q_{t,ml}$  is described by (2.21), the evolution of  $z_i$  is described by (2.22). So the basic equations of the model are:

$$\frac{d\theta_{v,ml}}{dt} = -\frac{\overline{w'\theta'_{v,z_i}} - \overline{w'\theta'_{v,0}}}{z_i}; \quad (3.1a)$$

$$\frac{dq_{t,ml}}{dt} = -\frac{\overline{w'q'_{t,z_i}} - \overline{w'q'_{t,0}}}{z_i}; \quad (3.1b)$$

$$\frac{dz_i}{dt} = w_e + w_{subs}. \quad (3.1c)$$

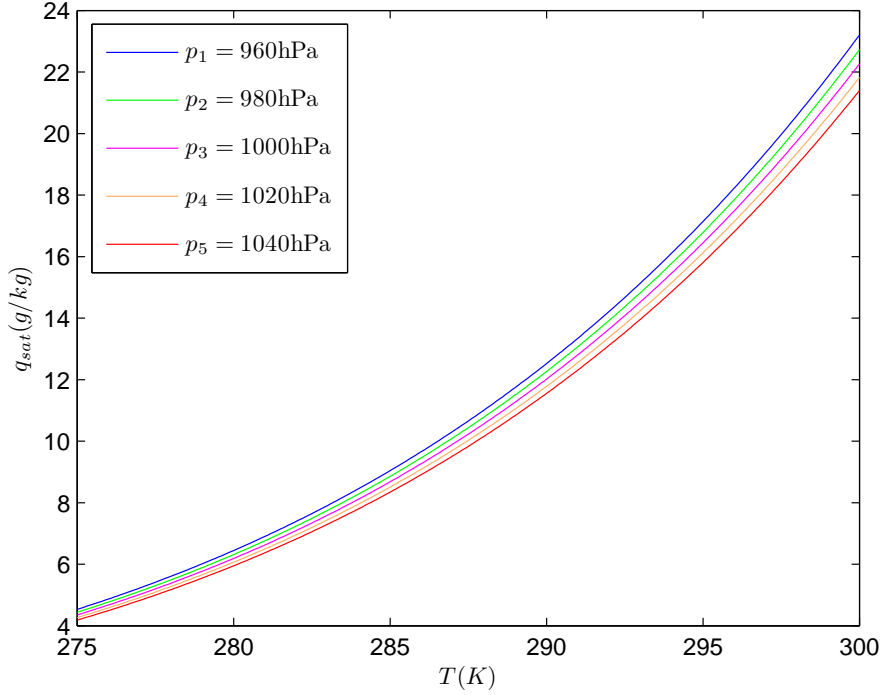


Figure 3.1: The humidity of saturation plotted as a function of  $T$  for 5 different values of the pressure.

In (3.1a) the variable  $\overline{w'\theta'_v}$  occurs. This variable is called the virtual potential temperature flux. In the next subsection we will see that the temperature fluxes at the top can be written in terms of the temperature fluxes at the surface. The temperature flux at the surface will be parameterized as a potential temperature flux and not as a virtual potential temperature flux. So the virtual potential temperature flux has to be related to the potential temperature flux  $\overline{w'\theta'}$ . This relation as derived in van der Dussen (2009) is:

$$\overline{w'\theta'_v} = \overline{w'\theta'} + 0.61\bar{\theta} \cdot \overline{w'q'_t}. \quad (3.2)$$

In the next subsection the entrainment rate will be parameterized. We have seen that entrainment is a buoyancy driven phenomenon. This implies that it depends on the difference in virtual potential temperature (which is a measure for buoyancy) between the mixed layer and the free atmosphere. This difference is denoted by  $\Delta\theta_v$  and is calculated as:

$$\Delta\theta_v = \theta_{fa} (1 + 0.61q_{t,fa}) - \theta_{ml} (1 + 0.61q_{t,ml}). \quad (3.3)$$

As we have seen earlier  $\theta_{fa}$  depends on the inversion height according to  $\theta_{fa}(z_i) = \theta_{fa}(z_i(0)) + \Gamma_\theta (z_i - z_i(0))$  so that we get:

$$\Delta\theta_v = \theta_{fa}(z_i(0)) + \Gamma_\theta (z_i - z_i(0)) (1 + 0.61q_{t,fa}) - \theta_{ml} (1 + 0.61q_{t,ml}). \quad (3.4)$$

## 3.2 Parameterizations

In system of equations (3.1) there are three equations in terms of more than three variables. Our goal is to find the evolution of  $\theta_v$ ,  $z_i$  and  $q_t$  so all variables have to be expressed in terms of these three variables so that system (3.1) can be solved. For the turbulent flux at  $z_i$  an approximate relation is derived by Lilly (1968):

$$\overline{w'\psi'_{z_i}} = -w_e \Delta\psi, \quad (3.5)$$

where  $\Delta\psi$  is the jump of  $\psi$  across the inversion. For the entrainment rate the parameterization of Moeng (2000) is used:

$$w_e = A \frac{\overline{w'\theta'_{v,0}}}{\Delta\theta_v}, \quad (3.6)$$

where the parameter  $A = 0.2$ . Now a relation has to be found for the surface fluxes. These fluxes are parameterized as follows:

$$\overline{w'\psi'_0} = C_D U (\psi_s - \psi_{ml}), \quad (3.7)$$

where  $\psi_s$  is the value of  $\psi$  at the surface,  $U$  is the wind speed and  $C_D$  is an exchange coefficient which is in good approximation equal to 0.001 Wakefield and Schubert (1981). The last unknown variable in system of equations (3.1) is the subsidence speed at the inversion. Inside free atmosphere the subsidence speed is proportional to the height according to  $w_{subs} = Dz$ , where  $D$  is called the large scale divergence, so at the inversion the subsidence speed is equal to:

$$w_{subs} = -Dz_i. \quad (3.8)$$

With these parameterizations system of equations (3.1) can be rewritten in a form where the only variables are  $\theta_{v,ml}$ ,  $z_i$  and  $q_{t,ml}$ .

## 3.3 Model parameters and initial conditions

With the three model equations written in terms of three variables the model parameters (such as  $T_s$  and  $\theta_{fa}(0)$ ) and three initial conditions have to be chosen. Before choosing these values it is necessary to look at the heat balance of the boundary layer. In figure 3.2 the heat balance in a slice of air with width  $\Delta x$  and height  $z_i$  is drawn schematically. We consider the slice to be moving with speed of the trade wind in the direction of the equator. The wind speed of the trade wind is denoted by  $U$ . As the slice moves southwards the sea surface temperature  $T_s$  will increase, this increase is about  $\delta T_s = 3 \cdot 10^{-6} \text{K/m}$  so  $T_s$  is calculated as:

$$T_s = T_s(0) + \delta T_s \cdot U \cdot t, \quad (3.9)$$

where  $t$  is the elapsed time. The initial potential temperature in the mixed layer ( $\theta_{ml}(0)$ ) is determined by a prescribed initial surface heat flux ( $H$ ). This heat flux is calculated as:

$$H = \rho c_p C_D U (T_s - T_{ml}(t=0, z=0)) = \rho c_p C_D U \frac{(\theta_s - \theta_{ml}(0))}{\Pi(p_{surf})}. \quad (3.10)$$

This heat flux is assumed to be linearly dependent on the wind speed, so that  $H = c_0 U + c_1$ . Furthermore it is assumed that for wind speeds considered in this thesis the transport from the surface to the atmosphere due to forced convection dominate over the rest of the forms of

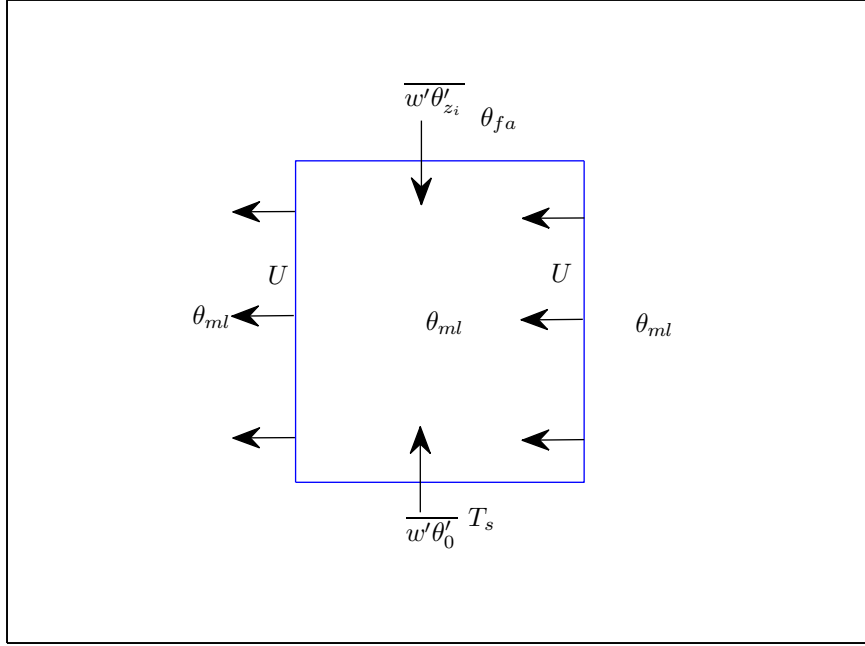


Figure 3.2: The heat balance of the boundary layer.

transport so that  $c_1 \approx 0$ . Thus  $\frac{H}{U}$  is constant. So  $\theta_{ml}(0)$  can be calculated using a reference value for the wind speed,  $U_{ref}$  at which the value of the initial heat flux is  $H_{ref}$ . This results in:

$$\theta_{ml}(0) = \theta_s - \frac{H_{ref}\Pi(p_{surf})}{U_{ref}\rho c_p C_D}. \quad (3.11)$$

The initial potential temperature just above the inversion ( $\theta_{fa}(0)$ ) is determined by a prescribed initial temperature jump ( $\Delta\theta(0)$ ) across the inversion so:

$$\theta_{fa}(0) = \Delta\theta(0) + \theta_{ml}(0). \quad (3.12)$$

The surface humidity ( $q_{t,s}$ ) is determined by the assumption that the air at the surface is saturated so that:

$$q_{t,s} = q_{sat}(T_s, p_{surf}). \quad (3.13)$$

The value of  $q_{sat}$  is of course calculated using the relationship of Clausius-Clapeyron. The initial mixed layer and free atmosphere humidities ( $q_{t,ml}(0)$  and  $q_{t,fa}(0)$ ) are determined in a similar way as the mixed layer and free atmosphere initial potential temperatures.  $q_{t,ml}(0)$  is determined by a prescribed initial latent heat flux  $LE$ .  $LE$  is calculated as:

$$LE = \rho L_v C_D U (q_{t,s} - q_{t,ml}), \quad (3.14)$$

here  $L_v$  is the latent heat of vaporization.  $LE$  is assumed to be linearly dependent on the wind speed according to  $LE = \frac{LE_{ref}}{U_{ref}} U$ , where  $LE_{ref}$  is the value of  $LE$  at wind speed  $U_{ref}$ . The result for the initial mixed layer humidity is:

$$q_{t,ml}(0) = q_{t,s} - \frac{LE_{ref}}{U_{ref}\rho L_v C_D}. \quad (3.15)$$

The initial free atmosphere humidity is determined by a prescribed initial humidity jump so:

$$q_{t,fa}(0) = \Delta q_t(0) + q_{t,ml}(0). \quad (3.16)$$

The last initial condition we need is the initial inversion height. This one is simply prescribed.





# Chapter 4

## Results

Now that the three model equations can be expressed in the three variables we are interested in, we can try to find a solution for the evolution of  $\theta_{v,ml}$ ,  $z_i$  and  $q_{t,ml}$ , given the appropriate initial conditions. With the evolution of these variables known, the evolution of  $q_{sat,top}$  can be calculated. With the evolution of both  $q_{t,ml}$  and  $q_{sat,top}$  known, the time after which saturation (and thus cloud formation) occurs, called  $t_s$ , can be calculated. Solving the system of equations analytically is very difficult if not impossible. Therefore the system is solved numerically using the Euler forward method. The system is solved for several initial values of  $\Delta\theta$  in the range of  $1K \leq \Delta\theta \leq 11K$  and initial values of  $\Delta q_t$  in the range of  $-q_{t,ml} \leq \Delta q_t \leq 0$ . Next a contourplot is made of  $t_s$  as a function of the initial temperature jump and the initial humidity jump. The contourplots are based on simulations of 10 hours. What happens after those 10 hours will be left out of consideration so the conclusion "no saturation" or "no cloud formation" means no saturation or no cloud formation within 10 hours. This procedure is repeated for several values of the wind speed, of the the large scale divergence and of the the initial inversion height. The value of the wind speed is varied in the range of  $3m/s \leq U \leq 15m/s$  and the value of the large scale divergence between  $0 \leq D \leq 1 \cdot 10^{-5}s^{-1}$ . The range of the values of  $z_{i,initial}$  will be discussed in the next subsection. The other parameters are fixed, their values are given in table 4.1

parameter	value
$T_s$	287K
$p_{surf}$	1020hPa
$A$	0.2
$LE_{ref}$	50W/m <sup>2</sup>
$H_{ref}$	10W/m <sup>2</sup>
$U_{ref}$	8m/s
$C_D$	0.001s <sup>-1</sup>
$\delta T_0$	$3 \cdot 10^{-6}K/m$

Table 4.1: The values of the parameters used in this research.

## 4.1 The influence of the initial inversion height

The start of the investigation to the influence of the inversion height is to determine for which values of  $z_{i,initial}$  the top of the mixed layer is saturated. This value of  $z_{i,initial}$  is called the critical value and is denoted by  $z_{i,crit}$ . As we have seen the initial value of  $\theta_{ml}$  is fixed. This implies that the initial value of  $q_{sat,top}$  is a function of  $z_{i,initial}$  only. The initial value of  $q_{t,ml}$  is also fixed. In figure 4.1 it can be seen, that the critical value of  $z_i$  with the parameters and initial conditions used is  $z_{i,crit} = 320\text{m}$ .

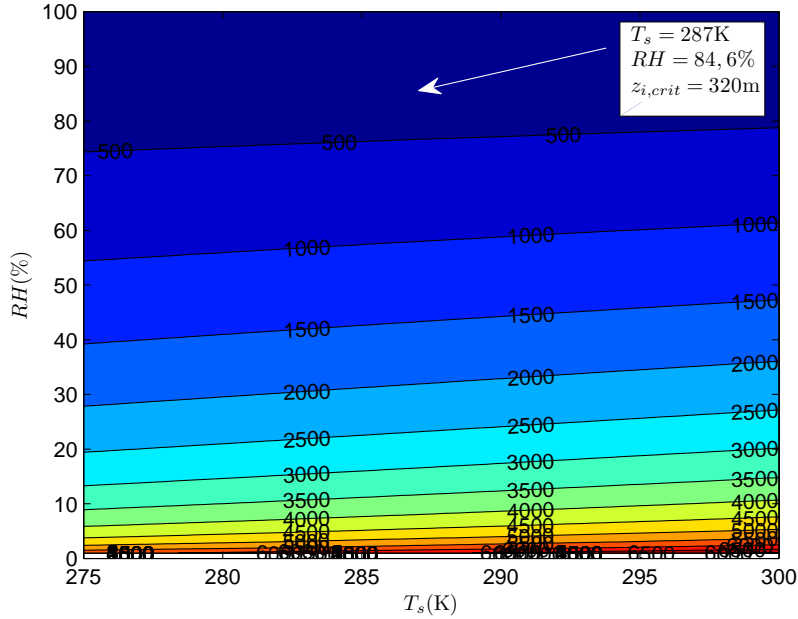
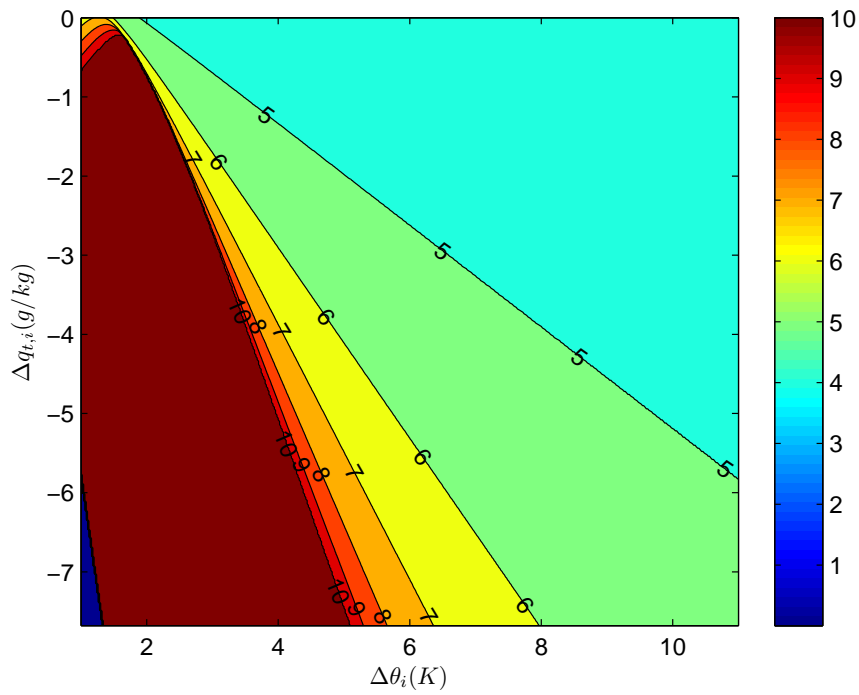
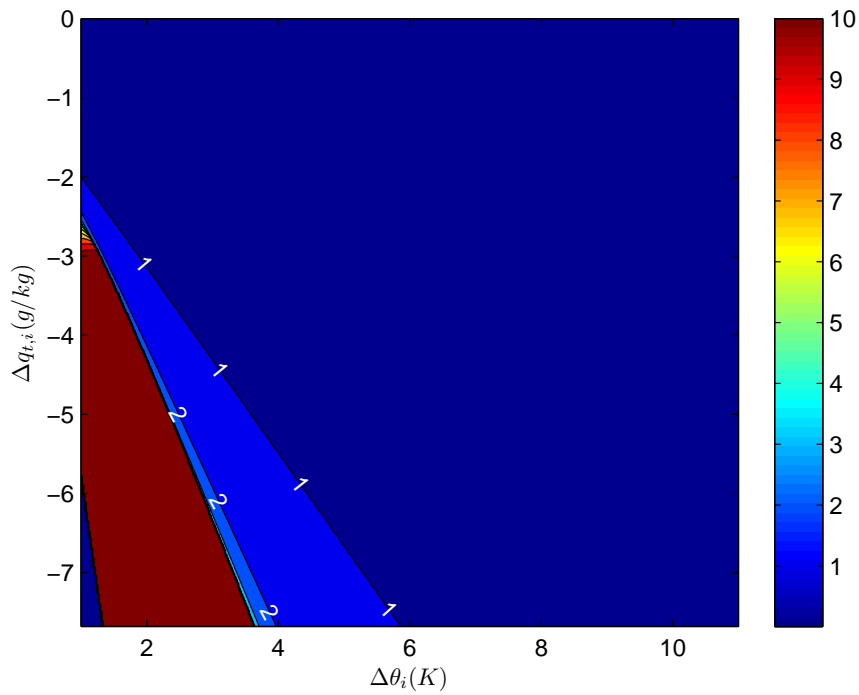


Figure 4.1: Contour plot of the critical values of  $z_i$  as a function of the sea surface temperature and the relative humidity at the bottom of the mixed layer.

Furthermore values of  $z_{i,initial}$  lower than 100m are left out of consideration, because inversion heights much lower than 100m don't occur in reality. To illustrate the influence of  $z_{i,initial}$  two contour plots are made. In the plots moderate values are chosen for  $U$  and  $D$ :



(a) Contour plot with  $z_{i,initial} = 100\text{m}$ ,  $U = 8\text{m/s}$ ,  $D = 5 \cdot 10^{-6}\text{s}^{-1}$ .



(b) Contour plot with  $z_{i,initial} = 300\text{m}$ ,  $U = 8\text{m/s}$ ,  $D = 5 \cdot 10^{-6}\text{s}^{-1}$ .

Figure 4.2: Contour plots of  $t_s$  in hours as a function of the initial values of  $\Delta\theta$  and  $\Delta q_t$ .

In figure 4.2 it can be seen, that for low initial values of  $z_i$  cloud formation takes a longer time than for high initial values. This makes sense because as values of  $z_i$  get higher the value of  $q_{sat,top}$  gets lower, so for higher values of  $z_i$  the top of the mixed layer is simply closer to saturation. A remarkable thing in both plots is the blue region they both have in the lower left corner. This region occurs in every situation considered. This is because of the low initial value of  $\Delta\theta_v$  in that region. Using (3.3)  $\Delta\theta_v$  can be written as:

$$\Delta\theta_v = (\Delta\theta + \theta_{ml})(1 + 0.61q_{t,fa}) - \theta_{ml}(1 + 0.61q_{t,ml}). \quad (4.1)$$

Now  $\Delta\theta_v$  can be calculated for a point inside the region. The initial value of  $\theta_{ml}$  is  $\theta_{ml} = 287.6\text{K}$ . If the initial values of  $\Delta\theta$  and  $\Delta q_t$  are  $\Delta\theta = 1\text{K}$  and  $\Delta q_t = -7.0\text{g/kg}$   $\Delta\theta$  is very small compared to  $\theta_{ml}$  so:

$$\Delta\theta_v \approx \Delta\theta + \theta_{ml}(1 + 0.61q_{t,fa} - 1 - 0.61q_{t,ml}) = \Delta\theta + 0.61\theta_{ml}\Delta q_t. \quad (4.2)$$

This means that the initial value of  $\Delta\theta_v$  under these circumstances is  $\Delta\theta_v \approx -0.23\text{K}$ . In this case the entrainment rate would be negative. This makes the mixed layer model invalid in these situations. Also when values of  $\Delta\theta_v$  get much lower than  $1\text{K}$  problems occur because of unrealistically high entrainment rates. Another remarkable thing is the sharp transition in figure 4.2(b) between the region on the left, where no clouds form, and the region on the right where cloud formation goes very quickly. The explanation of this will be given with help of figure 4.3.

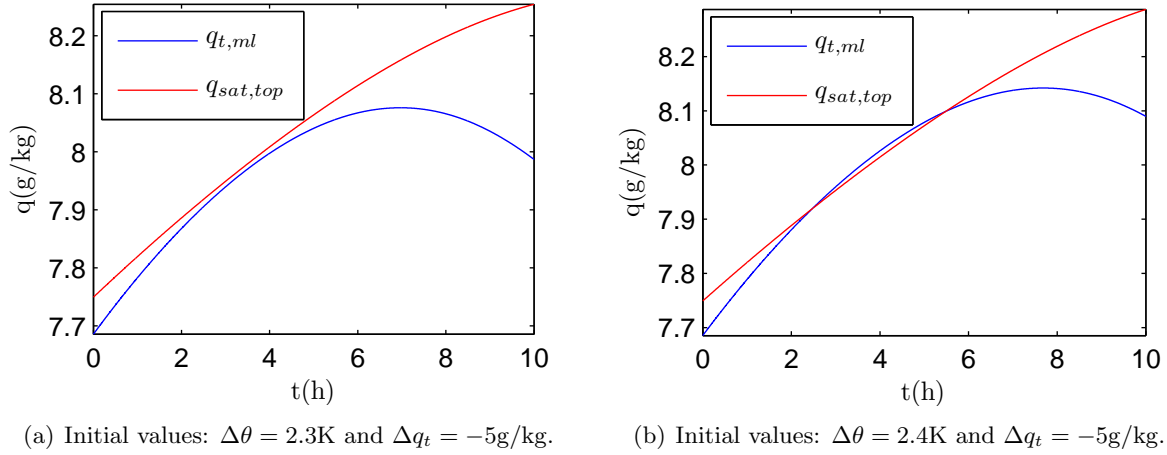


Figure 4.3: The evolution of  $q_{t,ml}$  and  $q_{sat,top}$  with  $z_{i,initial} = 300\text{m}$ ,  $U = 8\text{m/s}$  and  $D = 5 \cdot 10^{-6}\text{s}^{-1}$ .

In figure 4.3(a) it can be seen, that the graph  $q_{sat,top}$  just doesn't intersect the graph of  $q_{t,ml}$ . So in this situation no saturation occurs. In figure 4.3(b) the graph of  $q_{t,ml}$  does intersect the graph of  $q_{sat,top}$  so that in this situation saturation does occur, although the  $q_{t,ml}$  exceeds  $q_{sat,top}$  just a little bit and for a limited period of time so that cloud formation is not to be expected here. The transition seen in figure 4.2(b) is thus not as sharp as it appears. Furthermore it can be seen that  $q_{t,ml}$  shows a maximum. On this maximum value we have that  $\frac{dq_{t,ml}}{dt} = 0$ . Using (3.1a) it becomes clear that this implies that  $\overline{w'q'_{t,top}} = \overline{w'q'_{t,0}}$ . This is illustrated by figure 4.4

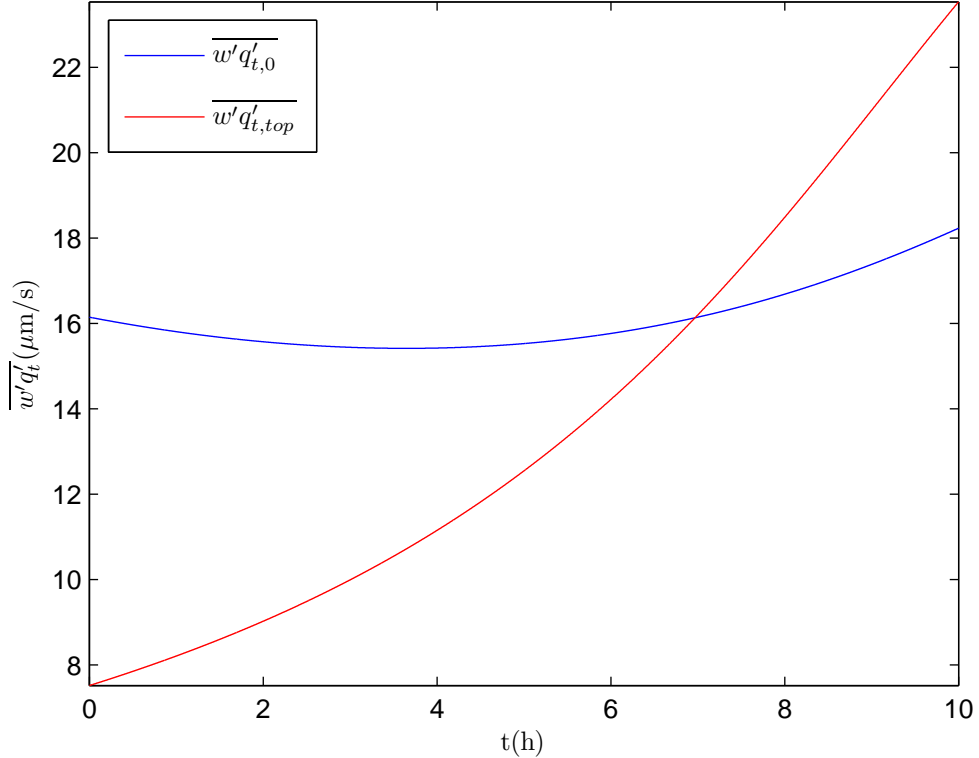


Figure 4.4: The evolution of  $\overline{w'q'_{t,top}}$  and  $\overline{w'q'_{t,0}}$  with  $U = 8\text{m/s}$   $D = 5 \cdot 10^{-6}\text{s}^{-1}$  and initial conditions  $z_i = 300\text{m}$ ,  $\Delta\theta = 2.3\text{K}$  and  $\Delta q_t = -5\text{g/kg}$ .

In the figure it can be seen that the surface flux is more or less constant, while the top flux increases rapidly. Based on (3.7) one might expect the surface flux to decrease because of the rising value of  $q_{t,ml}$ . The surface flux doesn't decrease, because the value of  $q_{t,s}$  rises. It rises due to the fact that the surface temperature increases with time, as we have seen in section 3.2. To explain the increase in the top flux we need (3.5) and (3.6), where in (3.5)  $\psi$  must be substituted by  $q_{t,ml}$ . Combining those equations we get

$$\overline{w'q'_{t,top}} = -A \frac{\overline{w'\theta'_{v,0}}}{\Delta\theta_v} \Delta q_t. \quad (4.3)$$

To find out which of the three variables on the right hand side is responsible for the increase of  $\overline{w'q'_{t,top}}$ , they have been plotted as a function of time in figure 4.5.

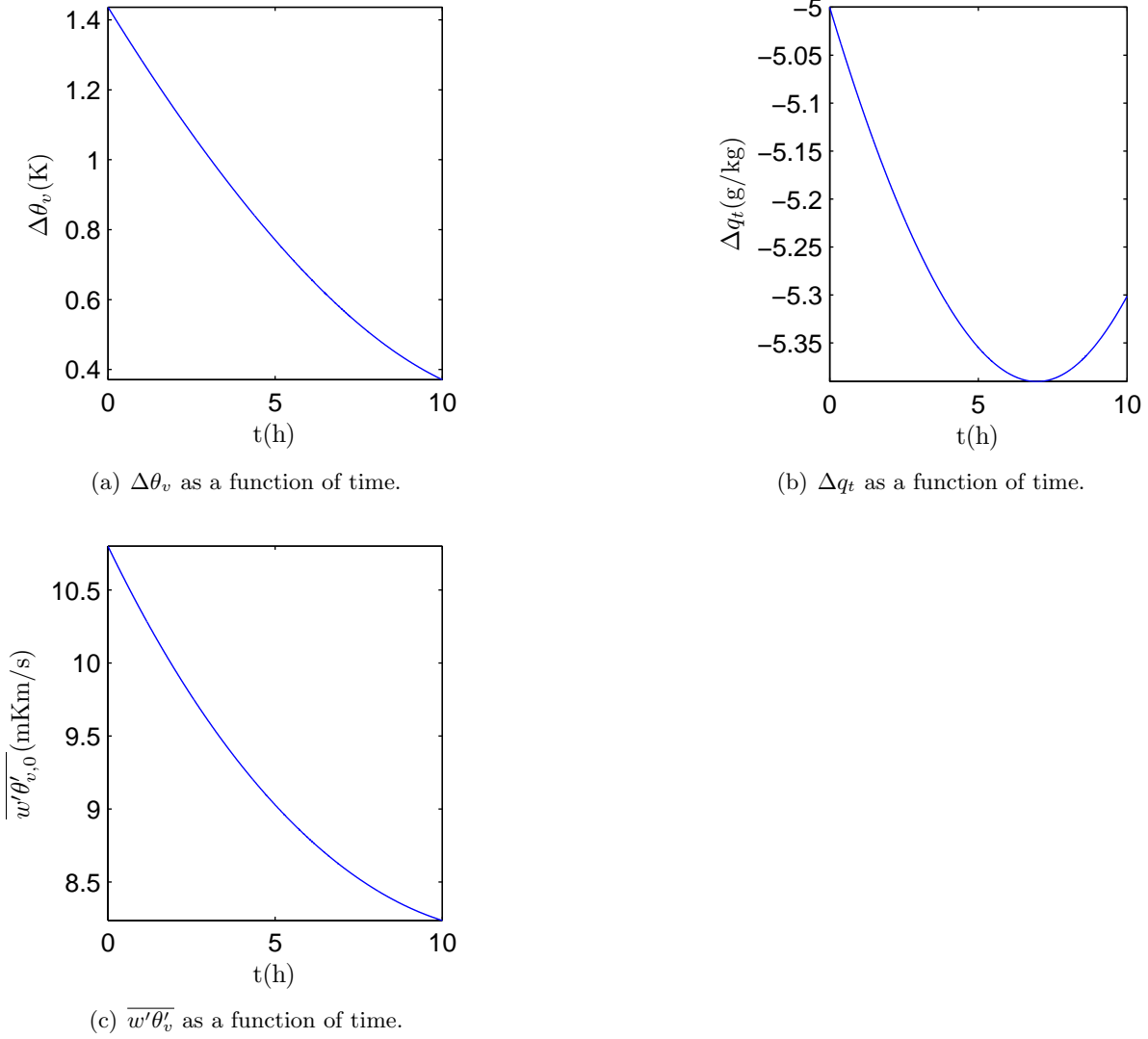


Figure 4.5: The evolution of  $\Delta\theta_v$ ,  $\Delta q_t$  and  $\overline{w'\theta'_{v,0}}$  with  $U = 8\text{m/s}$ ,  $D = 5 \cdot 10^{-6}\text{s}^{-1}$  and initial conditions  $z_i = 300\text{m}$ ,  $\Delta\theta_v = 2.3\text{K}$  and  $\Delta q_t = -5\text{g/kg}$ .

In figure 4.4 it can be seen that  $\overline{w'q'_{t,top}}$  after 10 hours is estimately three times as large as the initial value. Looking at (4.3) we see that  $\overline{w'q'_{t,top}}$  is proportional to  $\overline{w'\theta'_{v,0}}$  and  $\Delta q_t$  and inversly proportional to  $\Delta\theta_v$ . In figure 4.5 it can be seen that,  $\overline{w'\theta'_{v,0}}$  decreases and the absolute value of  $\Delta q_t$  increases but it increases by less than 10% after 7 hours, to decrease again afterwards. Those two thus don't explain the rapid increase of  $\overline{w'q'_{t,top}}$ . The value of  $\Delta\theta_v$  after 10 hours is less than the initial value divided by 3. As  $\Delta\theta_v$  is inversly proportional to  $\overline{w'q'_{t,top}}$  this leads to the conclusion that the main cause of the rapid increase of  $\overline{w'q'_{t,top}}$  is the decrease of  $\Delta\theta_v$ . Earlier in this section it is mentioned that when  $\Delta\theta_v$  gets much lower than 1K the mixed layer model may become invalid. This means that in this case the results for periods of more than 3 hours may not be reliable.

## 4.2 The influence of the wind speed

In the previous section it is mentioned that only initial inversion height of more than 100m are considered. For the lowest wind speed considered (3m/s) however an initial inversion height of at least 180m and absence of the large scale divergence is required to get cloud formation. For a large scale divergence of  $D = 5 \cdot 10^{-6}$  the minimal initial inversion height required to get clouds is 230m. To show the influence of the wind speed at low wind speeds two pairs of contour plots are made, one pair at  $z_{i,initial} = 300\text{m}$  and one pair at  $z_{i,initial} = 250\text{m}$ .

Looking at figure 4.6 in both cases three regions can be identified:

1. A region where no cloud formation occurs ( $t > 10\text{h}$ ).
2. A region where cloud formation occurs relatively quickly and the contour lines are widely separated. ( $t < 4\text{h}$ )
3. An intermediate region where the contour lines are close together. ( $4\text{h} < t < 10\text{h}$ )

It can be seen, that the position and the width of the intermediate region strongly depend on the wind speed. This is however only the case when the initial inversion height is such that the top of the mixed layer is almost saturated at the beginning. Figure 4.7 illustrates this.

The figure shows that both  $q_{t,ml}$  and  $q_{sat,top}$  are in good approximation linear functions of time. It can be seen, that when the wind speed increases the slope of both  $q_{t,ml}$  and  $q_{sat,top}$  increases. The slope of  $q_{t,ml}$  increases more than the slope of  $q_{sat,top}$ . So the wind causes the difference between the slope of  $q_{t,ml}$  and  $q_{sat,top}$  to increase, causing the time before they intersect to decrease (The intersection points are indicated by the black circles). Figure 4.7(a) corresponds to a point inside the intermediate region of figure 4.6(a) and figure 4.7(b) corresponds to a point inside the intermediate region of figure 4.6(b). In figure 4.7(b) it can be seen that a small increase of the slope of  $q_{t,ml}$  with respect to the slope of  $q_{sat,top}$  makes that the graphs, which do not intersect at  $U = 3\text{m/s}$  do intersect quite soon at  $U = 4\text{m/s}$ . This explains the large shift in the position of the intermediate region. To explain the increase of the width as the wind speed decreases knowledge of the influence of the initial values of  $\Delta\theta$  and  $\Delta q_t$  is required.

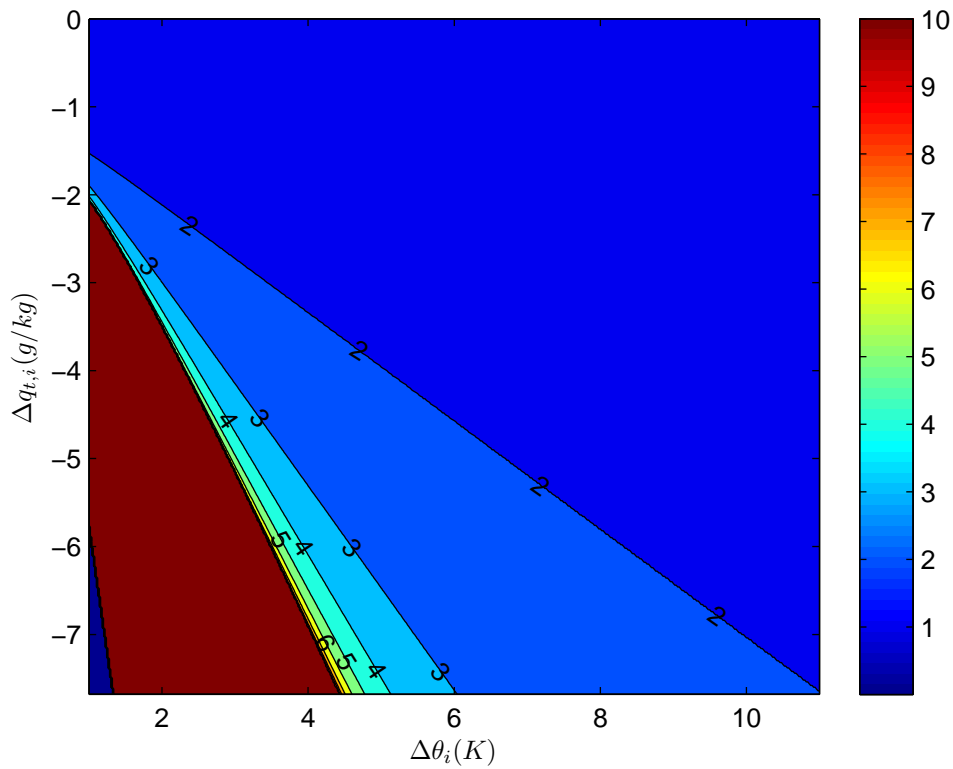
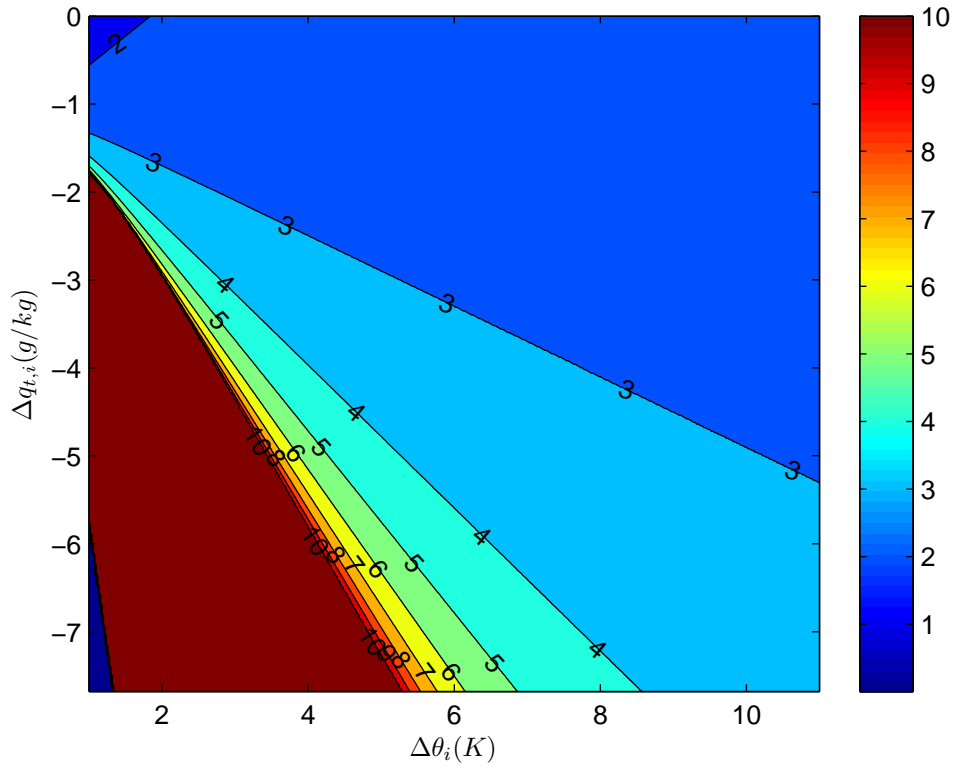


Figure 4.6: Contour plots of  $t_s$  as a function of the initial values of  $\Delta\theta$  and  $\Delta q_t$ , with  $z_{i,\text{initial}} = 300\text{m}$  and  $D = 5 \cdot 10^{-6}\text{s}^{-1}$ .



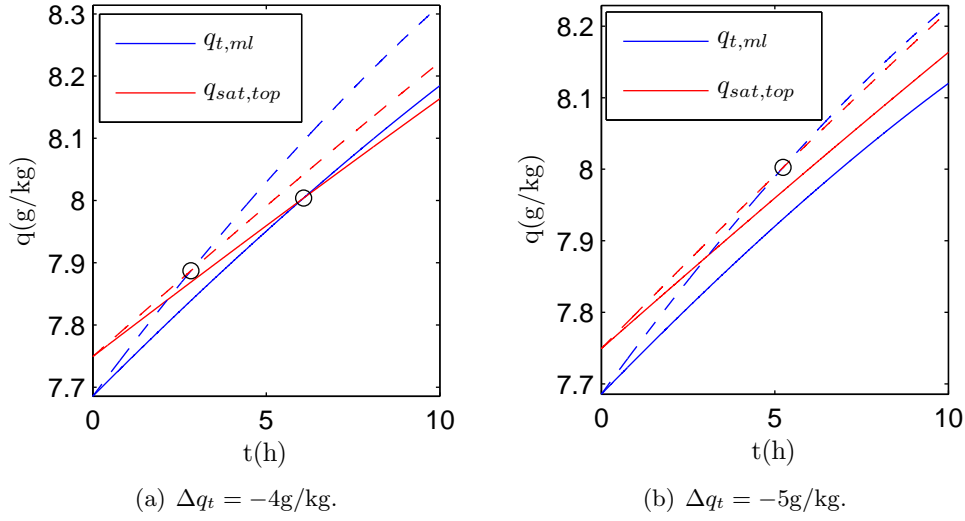


Figure 4.7: The evolution of  $q_{t,ml}$  and  $q_{sat,top}$  for  $U = 3\text{m/s}$  (solid line) and  $U = 4\text{m/s}$  (dashed line) with  $D = 5 \cdot 10^{-6}\text{s}^{-1}$  and initial conditions  $z_i = 300\text{m}$  and  $\Delta\theta = 3\text{K}$ .

In figure 4.8(a) it can be seen, that as the initial moisture jump gets smaller, the slope of  $q_{t,ml}$  gets larger while the slope of  $q_{sat,top}$  remains practically the same. Thus as the initial moisture jump gets smaller, clouds will form sooner. In figure 4.8(b) it can be seen that as the initial temperature jump increases, the time after which clouds occur decreases. In both subfigures of figure 4.8 we see that the slope of both  $q_{t,ml}$  and  $q_{sat,top}$  increases with increasing wind speed. Because of this the line segments towards the intersection point are longer. This makes a kind of leverage effect such that an increase of the slope of  $q_{t,ml}$  relative to the slope of  $q_{sat,top}$  makes the intersection point move more to the left for higher wind speeds. This is why the transition region is wider at lower wind speeds. For lower initial inversion heights the graphs of  $q_{t,ml}$  and  $q_{sat,top}$  start further separated from each other. This makes that the influence of a relative increase of the slope of one of the graphs decreases, so that the transition region gets stretched. In figure 4.9 it can be seen that for an initial inversion height of 250m the transition region gets so stretched that it in fact the three regions merge.

At higher wind speeds the sensitivity for the wind speed is much less as can be seen in figure 4.10

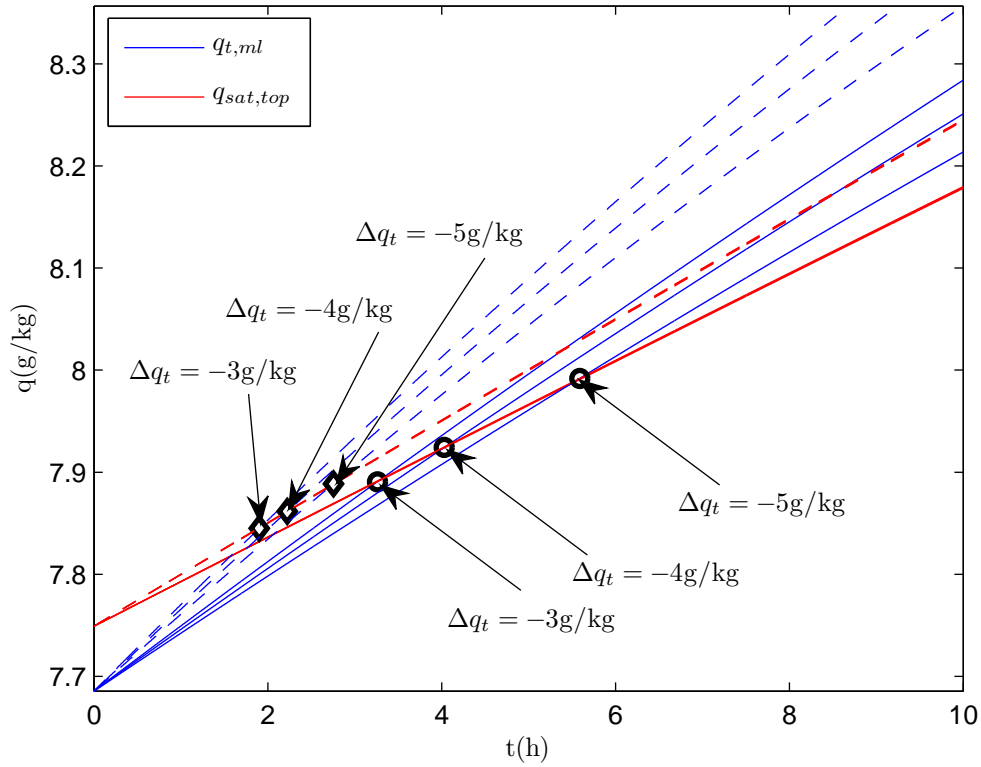
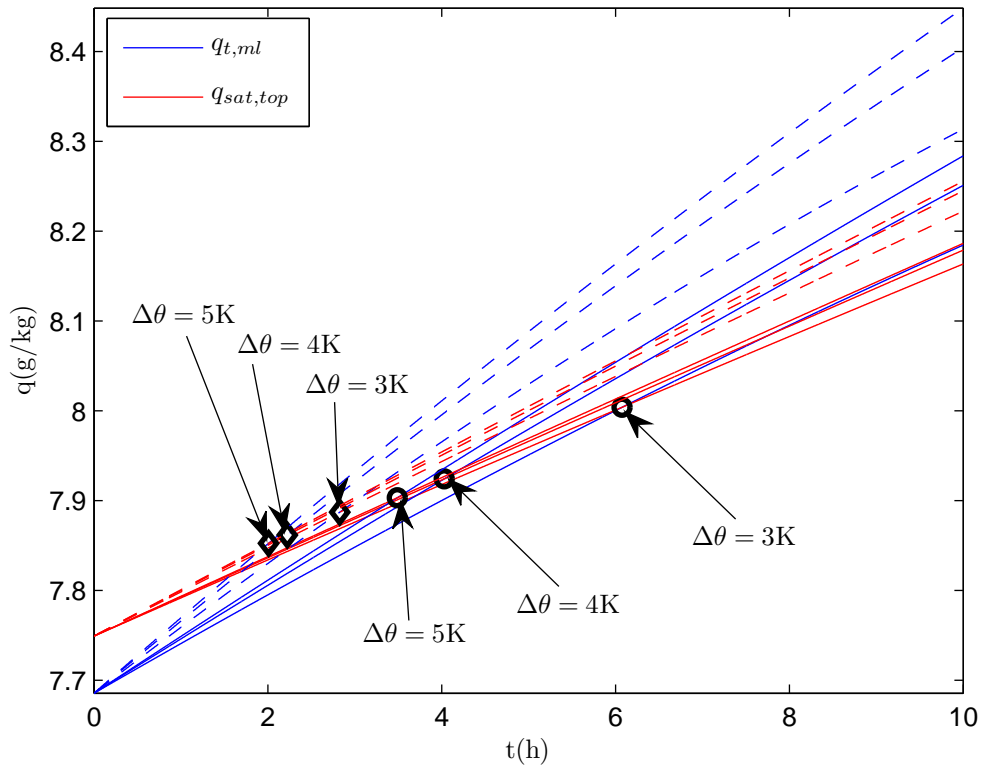
(a)  $\Delta\theta = 4\text{K}$ .(b)  $\Delta q_t = -5\text{g/kg}$ .

Figure 4.8: The evolution of  $q_t$  and  $q_{sat}$  for  $U = 3\text{m/s}$  (solid line) and  $U = 4\text{m/s}$  (dashed line) with  $D = 5 \cdot 10^{-6}\text{s}^{-1}$  and initial conditions  $z_i = 300\text{m}$  for various values of  $\Delta q_t$  and  $\Delta\theta$ . The circles indicate the intersection points of pairs of solid lines and the diamonds indicate the intersection points of pairs of dashed lines. The arrows indicate the initial value of  $\Delta q_t$  or  $\Delta\theta$  respectively belonging to the pair of lines it is pointing at.

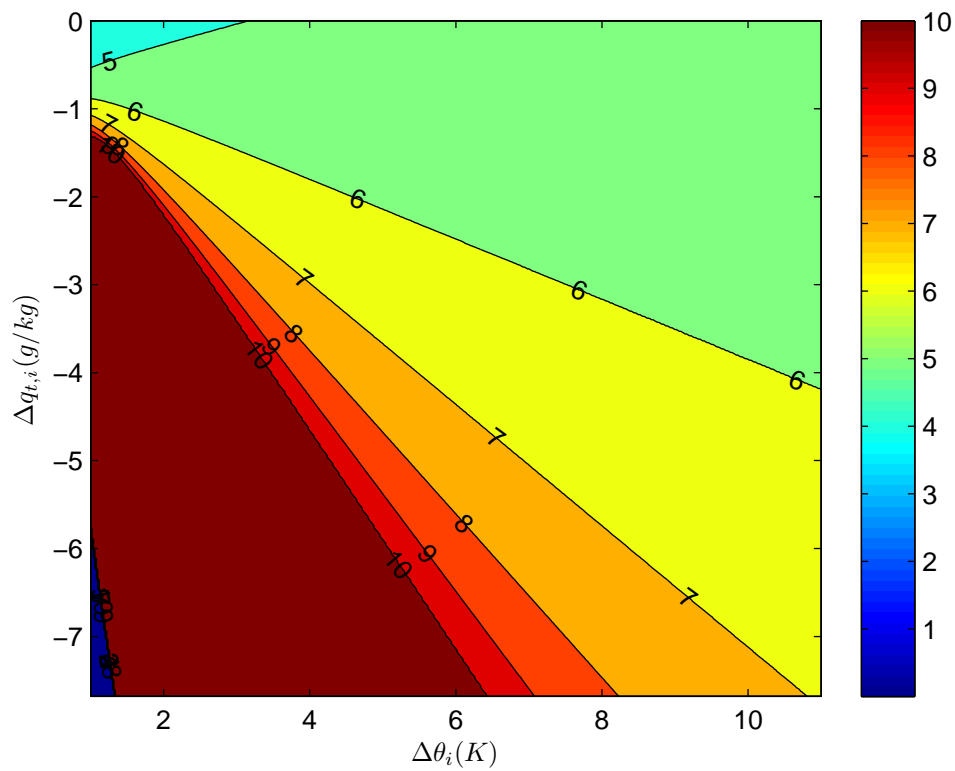
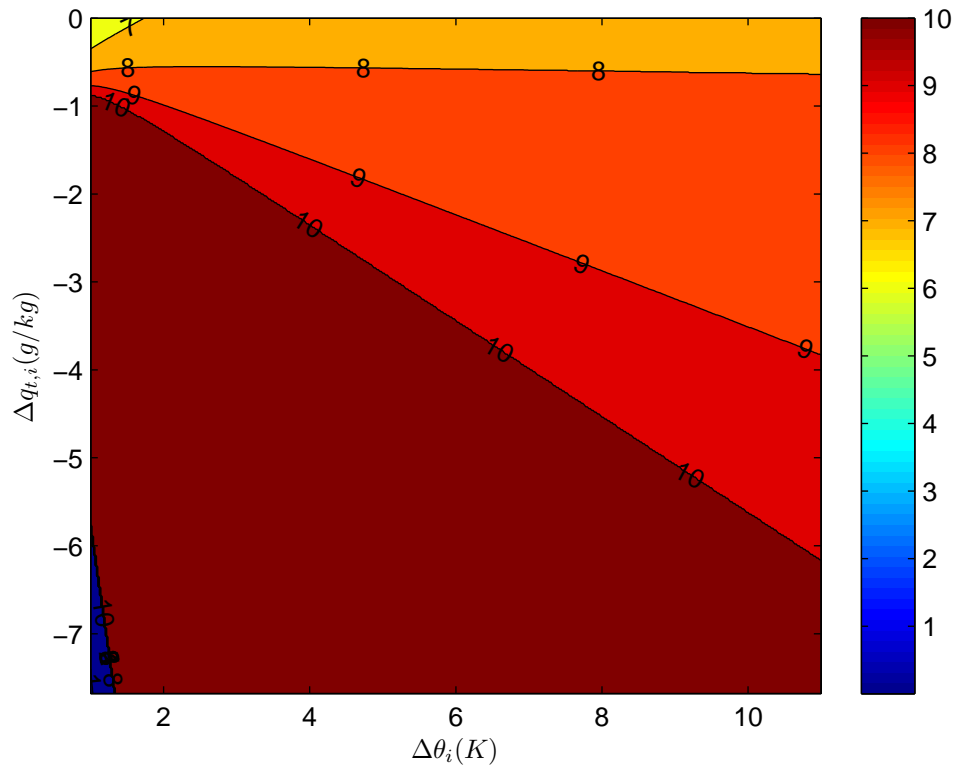


Figure 4.9: Contour plots  $t_s$  as a function of the initial values of  $\Delta\theta$  and  $\Delta q_t$ , with  $z_{i,initial} = 250\text{m}$  and  $D = 5 \cdot 10^{-6}\text{s}^{-1}$ .

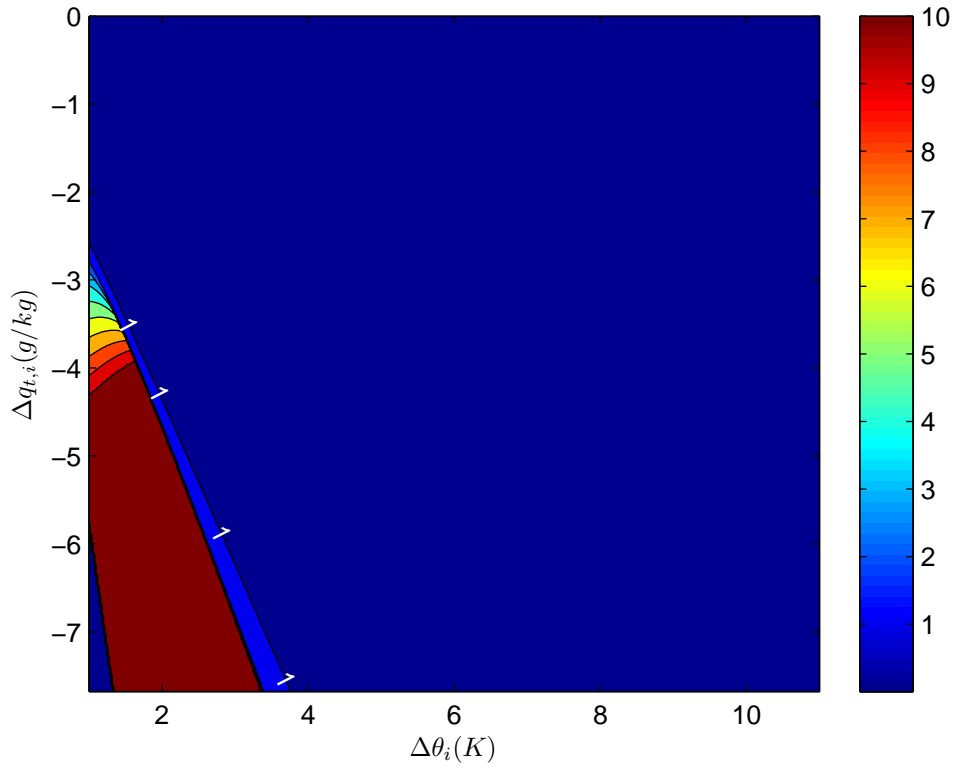
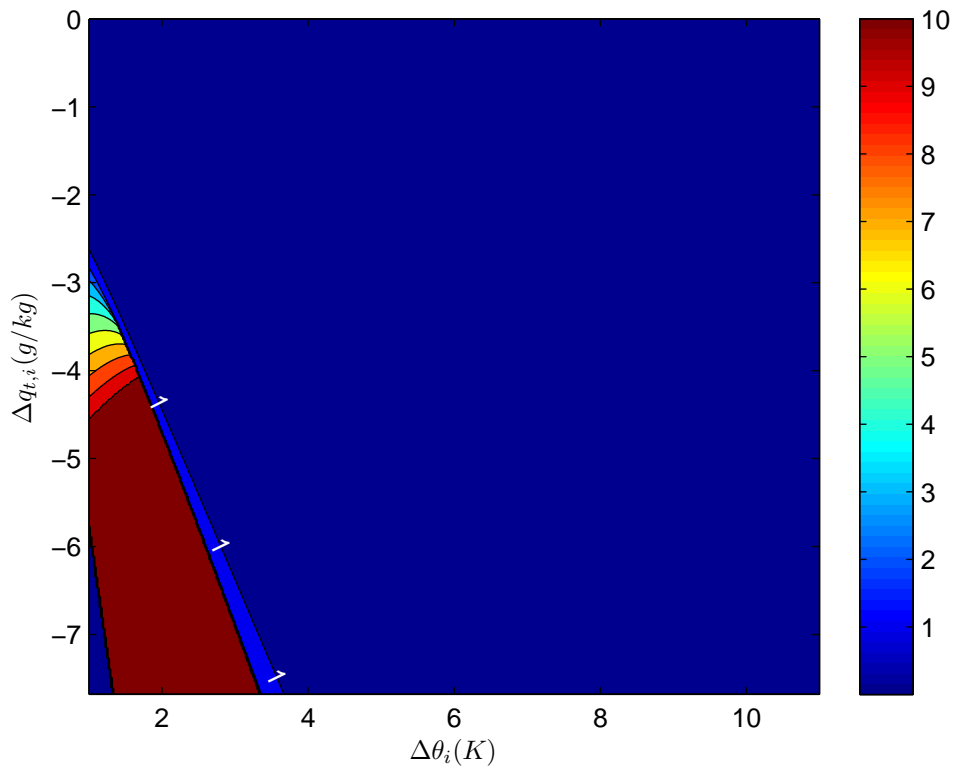
(a)  $U = 14$  m/s.(b)  $U = 15$  m/s.

Figure 4.10: Contour plots of  $t_s$  as a function of the initial values of  $\Delta\theta$  and  $\Delta q_t$ , with  $z_{i,initial} = 300$  m and  $D = 5 \cdot 10^{-6} \text{ s}^{-1}$ .

### 4.3 The influence of the large scale divergence

For the investigation to the influence of the large scale divergence a case similar to the case of figure 4.7 is used.

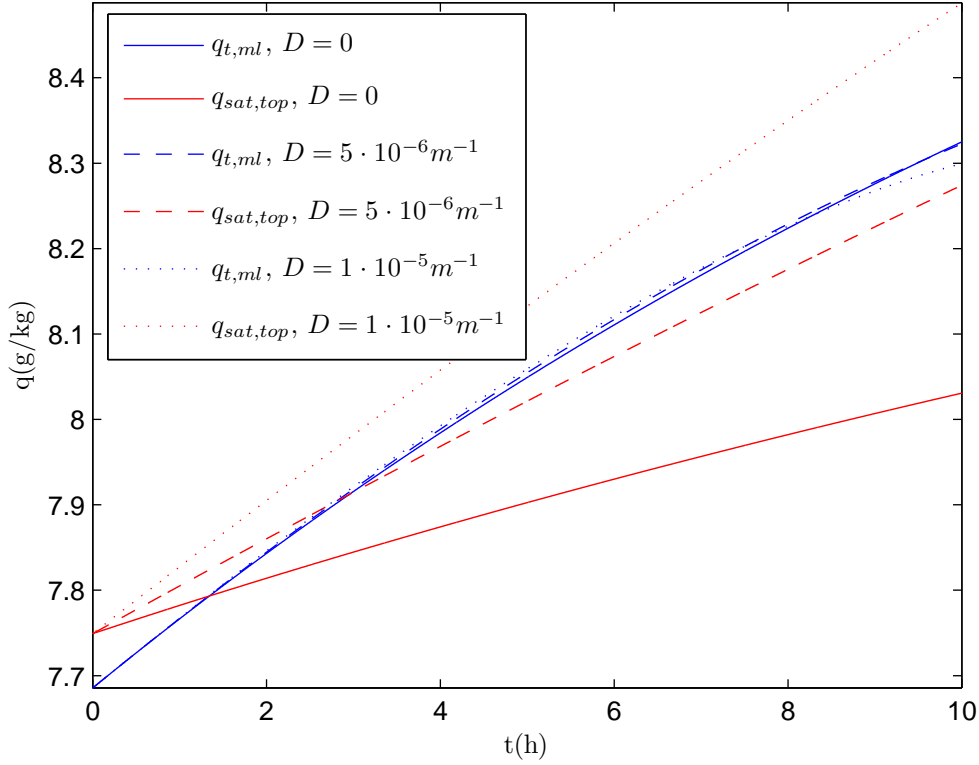


Figure 4.11: The evolution of  $q_t$  and  $q_{sat}$  with  $U=5\text{m/s}$  and initial conditions  $z_i = 300\text{m}$ ,  $\Delta\theta = 3\text{K}$  and  $\Delta q_t = -5\text{g/kg}$

Figure 4.11 shows that when the large scale divergence increases, the slope of the graph of  $q_{sat,top}$  increases relative to the slope of  $q_{t,ml}$ . So the large scale divergence has a similar effect on  $q_{sat,top}$  and  $q_{t,ml}$  as the windspeed has only the roles are reversed. Under these circumstances the time after which saturation occurs is thus strongly dependent on the large scale divergence, but the dependence is not as strong as the dependence on the wind speed.



## Chapter 5

# Conclusion

Looking at the contour plots shown in the previous chapter it can be observed that the time to reach saturation decreases as the moisture jump decreases. This can be explained looking at the moisture balance of the mixed layer. At the surface moisture is transported into the mixed layer causing the humidity to increase. At the top entrainment transports relatively dry air into the mixed layer causing the humidity to decrease. When the humidity jump at the top decreases the air entrained into the mixed layer becomes less dry so the decrease of humidity due to entrainment is less. Thus the humidity of the mixed layer tends to increase as the moisture jump decreases. Therefore a decrease of the humidity jump will lead to a decrease of the time after which saturation occurs. Another observation that can be made is that the time to reach saturation decreases as  $\Delta\theta$  increases. There are two major effects  $\Delta\theta$  has:

1. As  $\Delta\theta$  increases the air entrained into the mixed layer gets warmer.
2. An increase of  $\Delta\theta$  causes the entrainment rate to decrease according to  $w_e = A \frac{\overline{w'\theta'_v}}{\Delta\theta}$ .

The first effect makes that the mixed layer warms up faster causing  $q_{sat}$  to increase faster. The second effect makes that less warm, dry air is entrained into the mixed layer. So the second effect causes the tendency of the humidity to increase and weakens the first effect because less air is entrained. In figure 4.8(b) it can be seen that the initial value of  $\Delta\theta$  has a very small effect on  $q_{sat}$  compared to its effect on  $q_t$ . Thus the second effect almost neutralizes the first one and thereby causes the entrainment of dry air to decrease. So the net effect of an increase of  $\Delta\theta$  is that  $q_t$  increases while  $q_{sat}$  remains practically the same. This makes that cloud formation starts earlier if  $\Delta\theta$  increases. The general effect of the initial inversion height is that the lower it is, the higher the temperature at the top of the mixed layer. So as the initial inversion height gets lower, the initial value of  $q_{sat,top}$  gets higher, while the initial value of  $q_{t,ml}$  remains the same, so as the initial inversion height gets lower it takes longer before clouds start to form. The effects of the large scale divergence and the wind speed show a great similarity. They both affect the slope of the graphs of  $q_{sat}$  and  $q_t$ . the divergence has the strongest effect on  $q_{sat}$  and the wind speed on  $q_t$ . This explains their effect on the time after which saturation occurs. Their effect on this time is strongly dependent on the initial inversion height. Because both the divergence and the wind speed affect the slope of  $q_{sat}$  and  $q_t$  their influence on the time after which saturation occurs also depends on each other because of the leverage effect discussed in section 4.2. A remarkable effect is seen in figure 4.3. In this situation it is not really clear whether cloud formation will occur. The air gets saturated, but just a little saturation may not be enough to get cloud formation. Here the questions rise how much must  $q_t$  exceed  $q_{sat}$  to make the model used in this thesis invalid due to cloud formation and what will happen in that case? This could be topic of further study.





# Bibliography

- Lilly, D. K. (1968). Models of cloud-topped mixed layers under a strong inversion. *Quarterly Journal of the Royal Meteorological Society*, 94, 292–309.
- Moeng, C. H. (2000). Entrainment rate, cloud fraction, and liquid water path of planetary boundary layer stratocumulus clouds. *Journal of the Atmospheric Sciences*, 57, 3627–3643.
- Nieuwstadt, F. T. M. (1992). *Turbulentie*. Epsilon Uitgaven.
- Stull, R. B. (1993). *An Introduction to Boundary Layer Meteorology*. Kluwer Academic Publishers.
- van der Dussen, J. J. (2009). Large eddy and mixed-layer model simulations of the stratocumulus to cumulus transition as observed during ASTEX. Master’s thesis, Delft University of Technology.
- Wakefield, J. S. and W. H. Schubert (1981). Mixed-layer model simulation of eastern north pacific stratocumulus. *Monthly Weather Review*, 109, 1952–1968.



# Appendix A

## Validation

### A.1 The Nieuwstadt Case

If the subsidence is neglected and the surface heat flux is taken constant  $\Delta\theta$  can be written in terms of  $z_i$  and  $\Gamma_\theta$ . This is done in Nieuwstadt (1992). A quick derivation is given below. We start with (3.1a) and (3.1c). In absence of subsidence and using (3.6) we get:

$$\frac{d\theta_{v,ml}}{dt} = \frac{(A+1)\overline{w'\theta'_v}}{z_i} \quad (\text{A.1a})$$

$$\frac{dz_i}{dt} = \frac{A\overline{w'\theta'_v}}{\Delta\theta_v} \quad (\text{A.1b})$$

To obtain another equation for  $\Delta\theta$  the temperature profile of the free atmosphere,  $\theta_{v,fa} = \theta_{v,ml} + \Delta\theta + \Gamma_\theta(z_i(0) - z_i)$  is differentiated. Because there is no turbulence in free atmosphere the turbulent heat flux  $\overline{w'\theta'_v}$  is zero, so using (2.19) we get  $\frac{d\theta_{fa}}{dt} = 0$  so

$$\frac{d\Delta\theta_v}{dt} = \frac{d\Delta\theta_v}{dz_i} \frac{dz_i}{dt} = \Gamma_\theta \frac{dz_i}{dt} - \frac{d\theta_{v,ml}}{dt} \quad (\text{A.2})$$

Substitution of both equations of (A.1) into (A.2) gives:

$$\frac{d\Delta\theta_v}{dt} = \Gamma_\theta + \frac{1+A}{A} \frac{\Delta\theta_v}{z_i} \quad (\text{A.3})$$

The solution of this equation is:

$$\Delta\theta_v = \frac{A}{1+2A} \Gamma_\theta z_i + C z_i^{-\frac{1+A}{A}} \quad (\text{A.4})$$

Where  $C$  is a constant dependent on the initial inversion height  $z_i(0)$  and the initial temperature jump  $\Delta\theta(0)$ . This leads to the following expression:

$$\Delta\theta_v = \frac{A}{1+2A} \Gamma_\theta z_i + \left( \Delta\theta_v(0) - \frac{A}{1+2A} \Gamma_\theta z_i(0) \right) \left( \frac{z_i(0)}{z_i} \right)^{\frac{1+A}{A}} \quad (\text{A.5})$$

Now it can be checked whether the results of the program correspond to this equation. This is done in the figure below:

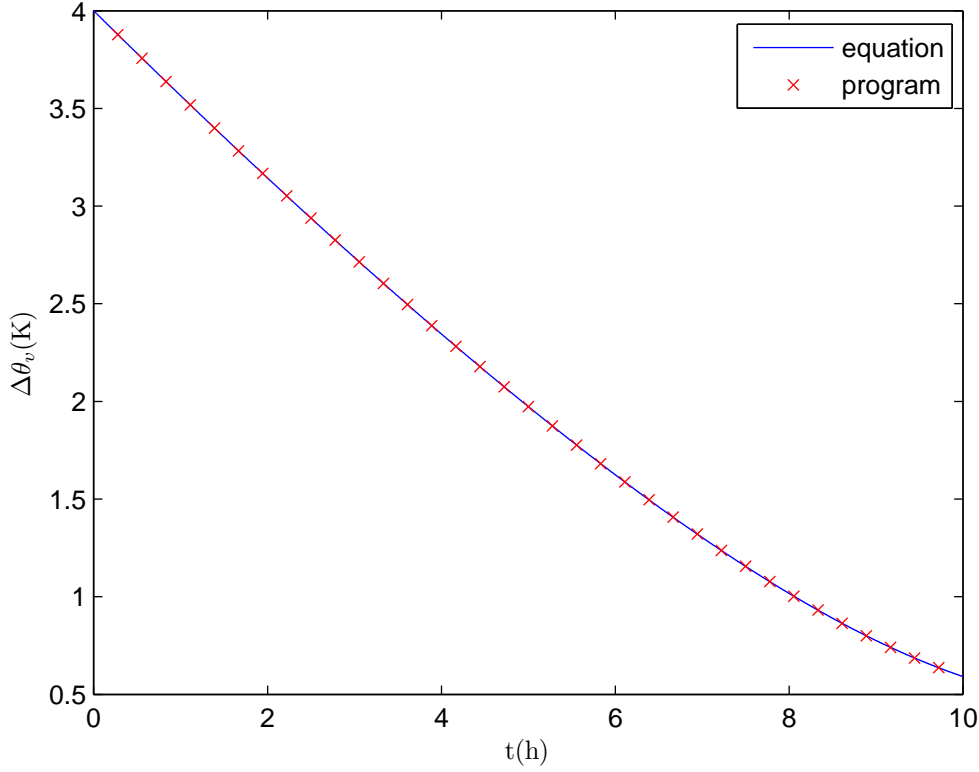


Figure A.1: Comparison of the evolution of  $\Delta\theta$  according to the program with the analytical result of Nieuwstadt (1992)

## A.2 Another analytical solution

The second relationship that has been derived is based on the assumption that  $\Gamma_\theta = 0$ . The derivation also starts with (3.1a) and (3.1c). Combining the two equations gives:

$$\frac{dz_i}{dt} = \frac{A}{A+1} \frac{z_i}{\Delta\theta_v} \frac{d\theta_{v,ml}}{dt} - Dz_i \quad (\text{A.6})$$

With the fact that  $\Gamma_\theta = 0$  we have that  $\Delta\theta_v = \theta_{v,fa} - \theta_{v,ml}$ , where  $\theta_{v,fa}$  is constant. So  $d\Delta\theta_v = -d\theta_{v,ml}$ . Thus (A.6) can be rewritten to:

$$\frac{1}{z_i} \frac{dz_i}{dt} = -\frac{A}{A+1} \frac{1}{\Delta\theta_v} \frac{d\Delta\theta_v}{dt} - D \quad (\text{A.7})$$

The solution of this equation is:

$$\ln |z_i| = -\frac{A}{A+1} \ln |\Delta\theta_v| - Dt + C_0 \quad (\text{A.8})$$

Knowing that at  $t = 0$   $z_i = z_i(0)$  and  $\Delta\theta_v = \Delta\theta_v(0)$  this can be written as:

$$\ln |z_i| = -\frac{A}{A+1} \ln \frac{|\Delta\theta_v|}{|\Delta\theta_v(0)|} - Dt \quad (\text{A.9})$$

With the fact that  $z_i > 0$  and  $\Delta\theta_v > 0$  we have:

$$z_i = z_i(0) \left( \frac{\Delta\theta_v}{\Delta\theta_v(0)} \right)^{-\frac{A}{A+1}} e^{-Dt} \quad (\text{A.10})$$

This analytical result is compared with the result of the program in the figure below.

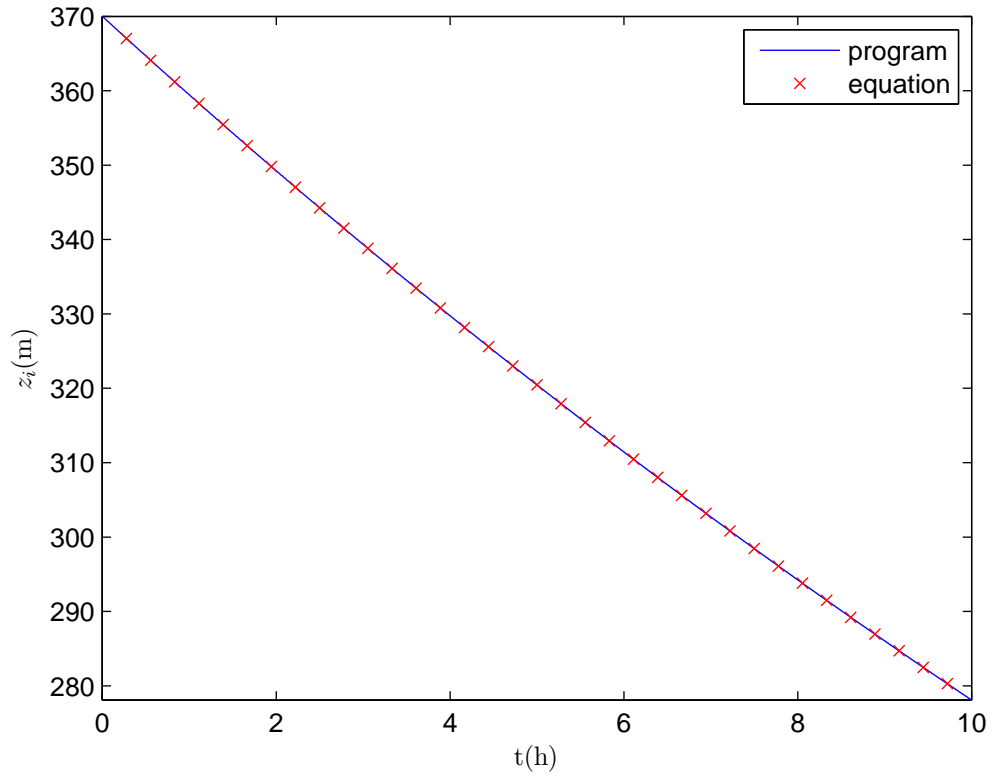


Figure A.2: Comparison of the evolution of  $\Delta\theta$  according to the program with the analytical result